Inorganic Chemistry
Article

Inorg. Chem. 2010, 49, 7721–7725 7721
DOI: 10.1021/ic100430g

Facile Synthesis and Luminescence of Uniform Y_2O_3 Hollow Spheres by a Sacrificial Template Route

Guang Jia, Hongpeng You,* Yanhua Song, Yeju Huang, Mei Yang, and Hongjie Zhang*

State Key Laboratory of Rare Earth Resource Utilization, Changchun Institute of Applied Chemistry, Chinese Academy of Sciences, Changchun 130022, P. R. China, and Graduate University of the Chinese Academy of Sciences, Beijing 100049, P. R. China

Received March 4, 2010

Uniform Y_2O_3 hollow microspheres have been successfully prepared via a urea-based homogeneous precipitation technique with colloidal melamine formaldehyde (MF) microspheres as templates followed by a subsequent calcination process. X-ray diffraction, energy dispersive X-ray analysis, and Fourier transform infrared spectroscopy results show that the MF templates can be effectively removed, and the amorphous precursor has converted to crystalline Y_2O_3 during the annealing process. Scanning electron microscopy and transmission electron microscopy images indicate that the Y_2O_3 hollow spheres inherit a spherical shape and good dispersion of MF templates, and the shell of the hollow spheres is composed of a large amount of uniform nanoparticles. The lanthanide activator ion Ln^{3+}-doped Y_2O_3 hollow microspheres exhibit bright down- and upconversion luminescence with different colors coming from different activator ions under ultraviolet or 980 nm light excitation, which may find potential applications in fields such as light phosphor powders, advanced flat panel displays, or drug delivery.

1. Introduction

Recently, much research attention has been paid to the synthesis of lanthanide compounds, because they can be used as high-performance phosphors, catalysts, and other functional materials as a result of their novel electronic, optical, and chemical properties arising from their 4f electrons.[1−6] It is well-known that the lanthanide oxides are very excellent host lattices for the luminescence of various optically active lanthanide ions.[7−9] Among them, yttrium oxide (Y_2O_3) is a promising host matrix for down- and upconversion luminescence due to its good chemical durability, thermal stability, and low phonon energy. The rare earth ion Ln^{3+}-doped Y_2O_3 materials have been proven to be important downconversion[10−13] and upconversion[14−16] phosphors. In particular, Y_2O_3:Eu^{3+} phosphor is a well-known red phosphor that is used in fluorescent lights, field emission displays, and cathode-ray tubes. To date, various morphologies of Y_2O_3 have been successfully prepared via different synthesis routes.[17−21] However, to our knowledge, little attention has been paid to the synthesis of uniform and well-defined Y_2O_3 hollow microspheres and their down- and upconversion luminescence properties. In addition, because the melamine formaldehyde resin is very cheap, hollow spherical phosphors would achieve a reduction in the amount of expensive rare earth materials, and thus lower the cost of the rare earth luminescent materials.

*To whom correspondence should be addressed. E-mail: hpyou@ciac.jl.cn (H.Y.); hongjie@ciac.jl.cn (H.Z.). Tel.: +86-431-85262798. Fax: +86-431-85698041.

(1) Palmer, M. S.; Neurock, M.; Olken, M. M. *J. Am. Chem. Soc.* **2002**, *124*, 8452.
(2) Cotter, J. P.; Fitzmaurice, J. C.; Parkin, I. P. *J. Mater. Chem.* **1994**, *4*, 1603.
(3) Eliseeva, S. V.; Bünzli, J. G. *Chem. Soc. Rev.* **2010**, *39*, 189.
(4) Wang, F.; Liu, X. G. *Chem. Soc. Rev.* **2009**, *38*, 976.
(5) Feng, W.; Sun, L. D.; Zhang, Y. W.; Yan, C. H. *Coord. Chem. Rev.* **2010**, *254*, 1038.
(6) Wang, X.; Li, Y. D. *Chem.—Eur. J.* **2003**, *9*, 5627.
(7) Mao, Y. B.; Tran, T.; Guo, X.; Huang, J. Y.; Shih, C. K.; Wang, K. L.; Chang, J. P. *Adv. Funct. Mater.* **2009**, *19*, 748.
(8) Jia, G.; Yang, M.; Song, Y. H.; You, H. P.; Zhang, H. J. *Cryst. Growth Des.* **2009**, *9*, 301.
(9) Jia, G.; Zheng, Y. H.; Liu, K.; Song, Y. H.; You, H. P.; Zhang, H. J. *J. Phys. Chem. C* **2009**, *113*, 153.
(10) Wu, C.; Qin, W.; Qin, G. *Appl. Phys. Lett.* **2003**, *82*, 520.
(11) Nelson, J. A.; Brant, E. L.; Wagner, M. J. *Chem. Mater.* **2003**, *15*, 688.
(12) Li, X.; Li, Q.; Xia, Z.; Wang, L.; Yan, W.; Wang, J.; Boughton, R. I. *Cryst. Growth Des.* **2006**, *6*, 2193.
(13) Sung, J. M.; Lin, S. E.; Wei, W. C. J. *J. Eur. Ceram. Soc.* **2007**, *27*, 2605.
(14) Qin, X.; Yokomori, T.; Ju, Y. *Appl. Phys. Lett.* **2007**, *90*, 073104.
(15) Chen, G. Y.; Liu, H. C.; Somesfalean, G.; Sheng, Y. Q.; Liang, H. J.; Zhang, Z. G.; Sun, Q.; Wang, F. P. *Appl. Phys. Lett.* **2008**, *92*, 113114.
(16) Glaspell, G.; Anderson, J.; Wilkins, J. R.; El-Shall, M. S. *J. Phys. Chem. C* **2008**, *112*, 11527.
(17) Qi, Z. M.; Shi, C. *Appl. Phys. Lett.* **2002**, *81*, 2857.
(18) Zhang, J.; Hong, G. *J. Solid State Chem.* **2004**, *177*, 1292.
(19) Alken, B.; Hsu, W. P.; Matijevic, E. *J. Am. Ceram. Soc.* **1988**, *71*, 845.
(20) Wang, H.; Lin, C.; Liu, X.; Lin, J. *Appl. Phys. Lett.* **2005**, *87*, 181907.
(21) Zeng, S.; Tang, K.; Li, T.; Liang, Z. *J. Colloid Interface Sci.* **2007**, *316*, 921.

Published on Web 08/10/2010

Generally, the properties of inorganic micro/nanostructures are fundamentally related to their chemical composition, crystal structure, surface chemistry, shape, and dimensionality.[22,23] Remarkably, hollow nano-/microspheres currently represent one of the fastest growing areas compared with other structural and geometrical features due to the distinct low effective density, high specific surface area, and encapsulation ability.[24] Recently, hollow spherical materials have found many applications in various fields such as photonic devices,[25] confined catalysis,[26] biotechnology,[27] electrochemical cells,[28] and drug delivery.[29] Many efforts have been made in the development of different methods for the design and fabrication of nano-/microscaled hollow spheres. Template-directed synthesis has been demonstrated to be an effective approach to prepare inorganic hollow spheres.[8,30] Among various hard templates, polymer latex particles, especially polystyrene (PS) beads, have been reported to be effective templates for the preparation of hollow spherical inorganic materials.[31] Recently, melamine formaldehyde (MF) colloidal particles which act as templates have been steadily employed to fabricate carbon spheres,[32] polyelectrolyte coated particles or hollow polymer capsules,[33] and core−shell structured particles.[34] However, to our knowledge, little attention has been paid to the preparation of hollow spherical inorganic compounds by using MF colloidal particles as templates. Compared with other hollow spherical functional materials, the rare earth oxide hollow spheres have been rarely studied. So it is desirable to develop facile and controllable methods for the synthesis of hollow spherical rare earth oxides with promising properties.

Li et al. have successfully prepared monodisperse $Y(OH)CO_3$ precursor and Y_2O_3 colloidal spheres via a urea-based homogeneous precipitation method.[35] Recently, we have synthesized the YPO_4 hierarchical hollow spheres by using the $Y(OH)CO_3$ precursor spheres as templates.[36] In the present study, we have utilized a homogeneous precipitation method to fabricate uniform and well-dispersed Y_2O_3 hollow microspheres with MF colloidal microspheres as templates followed by heat treatment. The phase structure, formation process, and luminescence properties of the as-synthesized hollow spheres have been investigated in detail.

2. Experimental Section

$Ln(NO_3)_3$ (Ln = Y, Eu, Yb, and Er) aqueous solutions were obtained by dissolving Ln_2O_3 (99.99%) in dilute HNO_3 solution under heating with agitation. All the other chemicals were analytical grade reagents and were used directly without further purification.

2.1. Synthesis. The monodisperse MF colloidal microspheres were prepared according to our previous report with a slight modification (reaction temperature: 80 °C).[34] In a typical synthesis of Y_2O_3 hollow spheres, 1.6 mmol of $Y(NO_3)_3$ aqueous solution was added to 30 mL of distilled water. Then 3.0 g of urea was dissolved in the solution by vigorous stirring to form a clear solution. Subsequently, the MF microspheres (0.2 g) were added and well dispersed into the above solution with the assistance of ultrasonication for 15 min. Finally, the mixture was transferred into a round-bottom flask and heated at 85 °C for 3 h with vigorous stirring. The precursor was collected by centrifugation and washed by deionized water and ethanol several times and dried at 60 °C in air. The final Y_2O_3 hollow microspheres were obtained through a heat-treatment at 800 °C for 2 h in air with a heating rate of 2 °C min^{-1}.

A similar process was employed to prepare Y_2O_3:5%Eu^{3+}, Y_2O_3:1%Er^{3+}, and Y_2O_3:10%Yb^{3+},1%Er^{3+} hollow microspheres by using a stoichiometric amount of $Eu(NO_3)_3$, $Er(NO_3)_3$, and/or $Yb(NO_3)_3$ aqueous solutions instead of $Y(NO_3)_3$ solution for the precursors at the initial stage as described above.

2.2. Characterization. The samples were characterized by powder X-ray diffraction (XRD) performed on a D8 Focus diffractometer (Bruker). Fourier transform infrared (FT-IR) spectra were obtained with a Perkin-Elmer 580B infrared spectrophotometer with the KBr pellet technique. Thermogravimetric analysis and differential scanning calorimetry (TG-DSC) data were recorded with a thermal analysis instrument (SDT 2960, TA Instruments, New Castle, DE) at a heating rate of 10 °C min^{-1}. The morphology and composition of the samples were inspected using a scanning electron microscope (SEM; S-4800, Hitachi) equipped with an energy-dispersive X-ray spectrometer (EDX; XFlash-Detector 4010, Bruker). Transmission electron microscopy (TEM) images and selected area electron diffraction (SAED) patterns were obtained by an FEI Tecnai G2 S-Twin transmission electron microscope with a field emission gun operating at 200 kV. Photoluminescence (PL) excitation and emission spectra were recorded with a Hitachi F-4500 spectrophotometer equipped with a 150 W xenon lamp as the excitation source. The luminescence decay curves were obtained from a Lecroy Wave Runner 6100 Digital Oscilloscope (1 GHz) using a tunable laser (pulse width = 4 ns, gate = 50 ns) as the excitation (Continuum Sunlite OPO). The upconversion (UC) emission spectra were obtained using a 980 nm laser from an OPO as the excitation source and detected by R955 (Hamamatsu) from 400 to 730 nm. All measurements were performed at room temperature.

3. Results and Discussion

3.1. Formation Process, Phase Identification, and Morphology. In this work, the homogeneous precipitation route was utilized to prepare uniform Y_2O_3 hollow microspheres with MF microspheres as templates. The whole

(22) Burda, C.; Chen, X.; Narayanan, R.; El-sayed, M. A. *Chem. Rev.* **2005**, *105*, 1025.
(23) Xia, Y. N.; Yang, P. D.; Sun, Y. G.; Wu, Y. Y.; Mayers, B.; Gates, B.; Yin, Y. D.; Kim, F.; Yan, Y. Q. *Adv. Mater.* **2003**, *15*, 353.
(24) (a) Zeng, H. *J. Mater. Chem.* **2006**, *16*, 649. (b) Hua, H.; Zeng, H. *Angew. Chem., Int. Ed.* **2004**, *43*, 5205. (c) Im, H. S.; Jeong, U.; Xia, Y. *Nat. Mater.* **2005**, *4*, 671.
(25) Xu, X. L.; Asher, S. A. *J. Am. Chem. Soc.* **2004**, *126*, 7940.
(26) Ikeda, S.; Ishino, S.; Harada, T.; Okamoto, N.; Sakata, T.; Mori, H.; Kuwabata, S.; Torimoto, T.; Matsumura, M. *Angew. Chem., Int. Ed.* **2006**, *45*, 7063.
(27) Wei, W.; Ma, G. H.; Hu, G.; Yu, D.; Mcleish, T.; Su, Z. G.; Shen, Z. Y. *J. Am. Chem. Soc.* **2008**, *130*, 15808.
(28) Lou, X. W.; Archer, L. A. *Adv. Mater.* **2008**, *20*, 1853.
(29) Yan, E.; Ding, Y.; Chen, C.; Li, R.; Hu, Y.; Jiang, X. *Chem. Commun.* **2009**, 2718.
(30) (a) Liang, H.; Zhang, H.; Hu, J.; Guo, Y.; Wan, L.; Bai, C. *Angew. Chem., Int. Ed.* **2004**, *43*, 1540. (b) Sun, X.; Li, Y. *Angw. Chem., Int. Ed.* **2004**, *43*, 3827. (c) Sun, Y. G.; Mayers, B. T.; Xia, Y. N. *Nano Lett.* **2002**, *2*, 481.
(31) (a) Yang, Z. Z.; Niu, Z. W.; Lu, Y. F.; Hu, Z. B.; Han, C. C. *Angew. Chem., Int. Ed.* **2003**, *42*, 1943. (b) Chen, M.; Wu, L. M.; Zhou, S. X.; You, B. *Adv. Mater.* **2006**, *18*, 801. (c) Hosein, I. D.; Liddell, C. M. *Langmuir* **2007**, *23*, 2892.
(32) Choi, W. S.; Koo, H. Y.; Kim, D. Y. *Langmuir* **2008**, *24*, 4633.
(33) (a) Choi, W. S.; Koo, H. Y.; Huck, W. T. S. *J. Mater. Chem.* **2007**, *17*, 4943. (b) Zheng, S. P.; Tao, C.; He, Q.; Zhu, H. F.; Li, J. L. *Chem. Mater.* **2004**, *16*, 3677.
(34) Jia, G.; Liu, K.; Zheng, Y. H.; Song, Y. H.; You, H. P. *Cryst. Growth Des.* **2009**, *9*, 3702.
(35) (a) Li, J. G.; Li, X. D.; Sun, X. D.; Ikegami, T.; Ishigaki, T. *Chem. Mater.* **2008**, *20*, 2274. (b) Li, J. G.; Li, X. D.; Sun, X. D.; Ishigaki, T. *J. Phys. Chem. C* **2008**, *112*, 11707.
(36) Zhang, L. H.; Jia, G.; You, H. P.; Liu, K.; Yang, M.; Song, Y. H.; Zheng, Y. H.; Huang, Y. J.; Guo, N.; Zhang, H. J. *Inorg. Chem.* **2010**, *49*, 3305.

Scheme 1. Schematic Illustration for the Overall Formation Process of Y_2O_3 Hollow Microspheres

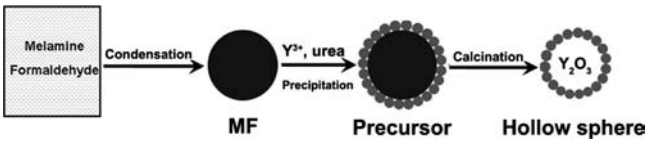

synthetic process can be summarized by the following steps:

(a) Preparation of uniform MF microspheres via a condensation process in aqueous solution;[32,34]
(b) Synthesis of core−shell-structured precursor by a homogeneous precipitation method;
(c) Calcination of the precursor to remove the MF cores and make the precursor shell decompose, thus resulting in Y_2O_3 hollow spheres.

A schematic illustration for the overall formation process of the uniform Y_2O_3 hollow spheres is presented in Scheme 1. The MF colloidal microspheres consist of a large amount of hydrophilic functional groups, so the MF templates are hydrophilic and may have a good affinity with Y^{3+}, OH^-, and CO_3^{2-} (OH^- and CO_3^{2-} releasing from urea) in aqueous solution. During the formation process of the precursor, the as-formed $Y(OH)CO_3$ nuclei may be easily absorbed on the surface of the hydrophilic MF microspheres. As the reaction proceeded, the amorphous precursor nuclei continued to grow and served as the seeds for the growth of $Y(OH)CO_3$ nanoparticles on the surface of the MF templates. In the calcination process, the MF cores were burned out and the amorphous $Y(OH)CO_3$ shell converted into crystalline Y_2O_3, resulting in the formation of the uniform Y_2O_3 hollow spheres.

Figure 1 shows the X-ray diffraction patterns of the as-formed precursor, the pure and Ln^{3+}-doped Y_2O_3 after calcination at 800 °C. It can be seen that no obvious diffraction peak appears for the precursor, indicating that the precursor is amorphous before calcination. The component of the amorphous precursor can be confirmed to be $Y(OH)CO_3$ according to previous reports.[8,35] After annealing at 800 °C for 2 h, all the diffraction peaks of the pure and Ln^{3+}-doped products can be indexed well to the cubic phase of Y_2O_3 [JCPDS No. 65-3178; space group: $Ia\bar{3}(206)$] (Figure 1b−e). One can also observe that the diffraction peaks of the as-obtained Y_2O_3 and Ln^{3+}-doped Y_2O_3 samples are very sharp and strong, indicating that the Y_2O_3 product with high crystallinity can be synthesized by this method. This is important for phosphors, because high crystallinity generally means less traps and stronger luminescence. As the ionic radius of Y^{3+} is smaller than that of Eu^{3+} and bigger than those of Yb^{3+} and Er^{3+} ions, the diffraction peaks of the Y_2O_3:5% Eu^{3+} sample shifts to the lower angle side and the Y_2O_3:1%Er^{3+} and Y_2O_3:10%Yb^{3+},1%Er^{3+} samples shift slightly to the higher angle side in contrast with that of the undoped Y_2O_3 sample. The result indicates that the activator ions have been effectively doped into the Y_2O_3 host lattice.

The thermal behaviors of the as-prepared precursor were investigated by TG-DSC measurements (Figure 2). There are two major stages of sharp weight loss in the TG curve at 410 and 493 °C, accompanying their corresponding exothermic peaks in the DSC curve (red line). The two rapid weight losses can be assigned to the dehydration and burning of the MF templates, respectively. In addition, a slight weight loss accompanied with a broad endothermic peak can be observed from 600 to 800 °C, which can be assigned to the conversion from the amorphous precursor to the crystalline Y_2O_3. The residual weight percentage of the precursor is about 30.5%, which accounts for the final Y_2O_3 product.

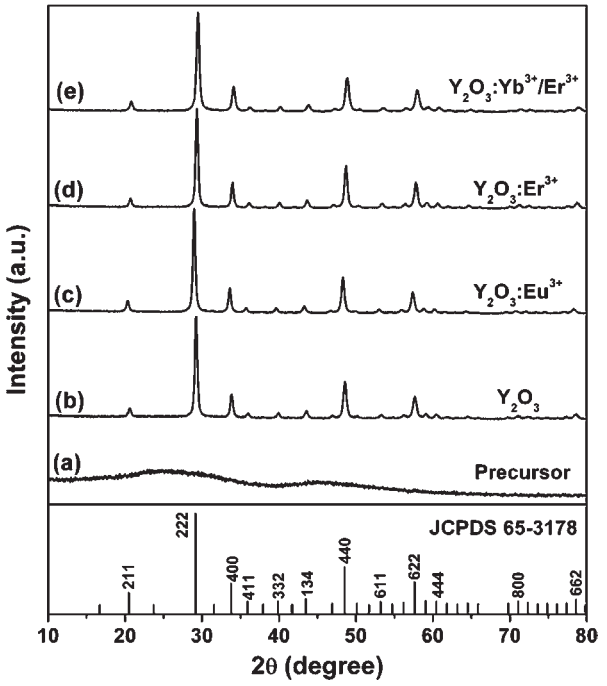

Figure 1. XRD patterns of the samples for (a) as-formed precursor and (b) Y_2O_3, (c) Y_2O_3:5%Eu^{3+}, (d) Y_2O_3:1%Er^{3+}, and (e) Y_2O_3:10% Yb^{3+},1%Er^{3+} after calcination at 800 °C for 2 h. The standard data for cubic phase Y_2O_3 (JCPDS No. 65-3178) is presented as a reference.

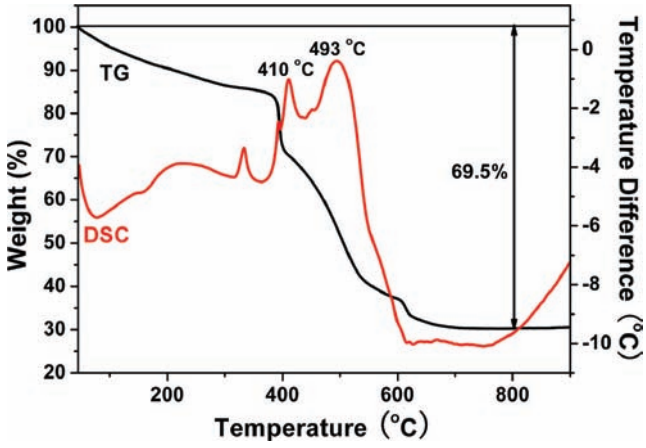

Figure 2. TG-DSC curves of the core−shell-structured precursor.

Figure 3a shows the SEM image of the bare MF microspheres. One can observe that the MF templates consist of highly uniform and well-dispersed microspheres with diameters of about 2.3 μm. It can also be seen that the surfaces of the monodisperse MF microspheres are very smooth. Figure 3b shows the SEM image of the precursor before calcination. The uniform composite microspheres inherit the spherical morphology

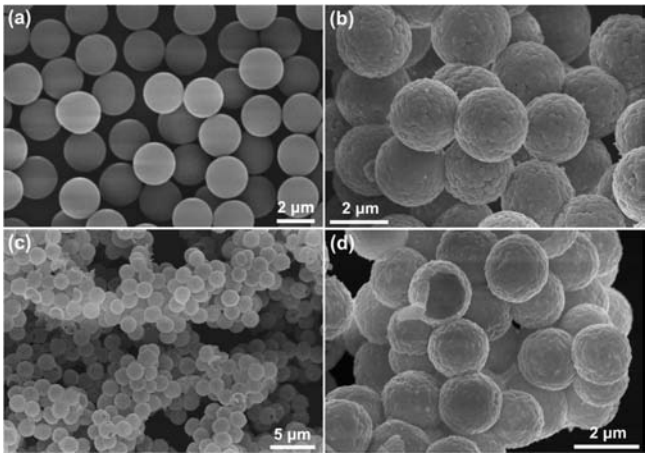

Figure 3. SEM images of (a) MF microspheres, (b) core−shell-structured precursor, and (c, d) Y_2O_3 hollow microspheres.

and the good dispersion of the MF templates, but the surfaces of precursor particles are much rougher than that of bare MF cores due to the precipitation of a large amount of uniform $Y(OH)CO_3$ nanoparticles. Naturally, the size of the core−shell-structured particles is a little larger than that of pure MF microspheres because of the amorphous shell. Figure 3c,d shows the morphology of the Y_2O_3 sample after calcination at 800 °C. A panoramic SEM image demonstrates that the Y_2O_3 sample consists of a large scale of uniform and well-dispersed hollow spheres (Figure 3c), which implies that the MF templates essentially determine the shape and structure of the final products. In addition, it can be seen that the average diameters of the Y_2O_3 hollow spheres decrease in comparison with those of the precursor microspheres. The shrinkage can be attributed to the dehydration of the cross-linked MF templates and the conversion from the loosely composite precursor to compact oxides in the outer shell. The ruptured hollow microspheres (Figure 3d) indicate that the microspheres are of hollow structures and the thickness of the shell is about 100 nm. The rupture of the microspheres can be attributed to releasing of gaseous carbon/nitrogen oxides when the burning of MF templates occurred during the annealing process.

Figure 4 shows the TEM images of the Y_2O_3 hollow spheres. The TEM images exhibits uniform spherical morphology and good dispersion. The strong contrast between the dark edge and the pale center is direct evidence of the hollow nature of the microspheres (Figure 4a). The average size of the hollow spheres and the thickness of the shells are about 1.8 μm and 100 nm, which are in agreement with the SEM images (Figure 3c,d). As can be seen from the enlarged TEM image, the shells of the hollow spheres are composed of uniform nanoparticles (Figure 4b). It should be noted that the morphologies of the as-synthesized Eu^{3+}, Er^{3+}, and/or Yb^{3+}-doped Y_2O_3 hollow spheres are similar to that of the Y_2O_3 sample.

The Eu^{3+}-doped precursor and final product were taken as an example to investigate the element composition by EDX spectra. The EDX analysis indicates that the MF templates have been removed completely and the precursor shell has converted to crystalline Y_2O_3 during the calcination process (Figure S1 in the Supporting Information). In addition, the FT-IR spectra were used

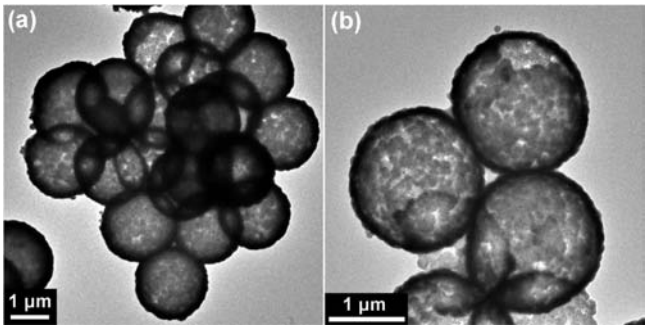

Figure 4. (a, b) TEM images of the Y_2O_3 hollow microspheres.

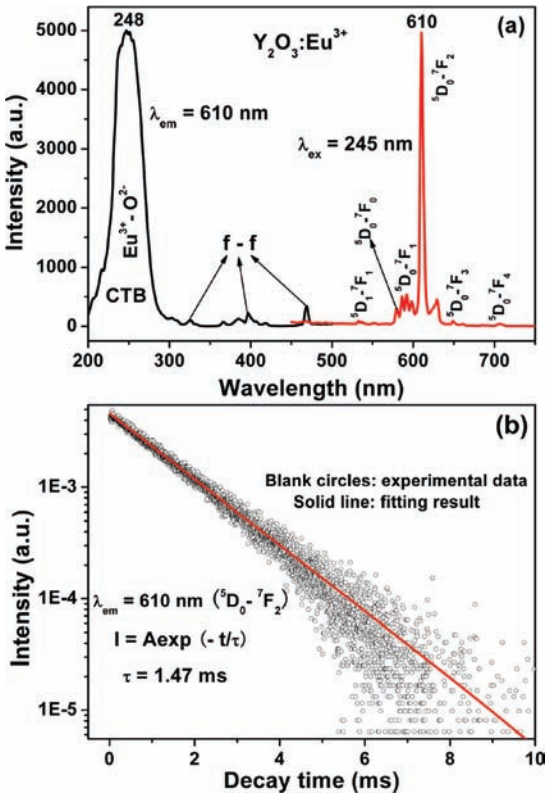

Figure 5. (a) PL excitation and emission spectra and (b) decay curve of Y_2O_3:5%Eu^{3+} hollow microspheres.

to identify the functional groups of the MF template, the core−shell-structured precursor, and the final Y_2O_3 product (Figure S2 in the Supporting Information). The FT-IR result provides additional evidence that the MF template can be effectively removed during the calcination process, which agrees well with the XRD and EDX results. The detailed discussion for the EDX and FT-IR analysis are presented in the Supporting Information.

3.2. Luminescence Properties. It is well-known that the yttrium oxide (Y_2O_3) is an excellent host lattice for both downconversion and upconversion luminescence of various optically active rare earth ions due to its favorable physical properties. In our case, a stoichiometric amount of lanthanide ions (Eu^{3+}, Er^{3+}, and Yb^{3+}) were doped into the Y_2O_3 host lattice to investigate the luminescence properties.

Figure 5a shows the excitation and emission spectra of as-prepared Y_2O_3:Eu^{3+} hollow spheres. The excitation spectrum consists of a strong broadband at about 248 nm

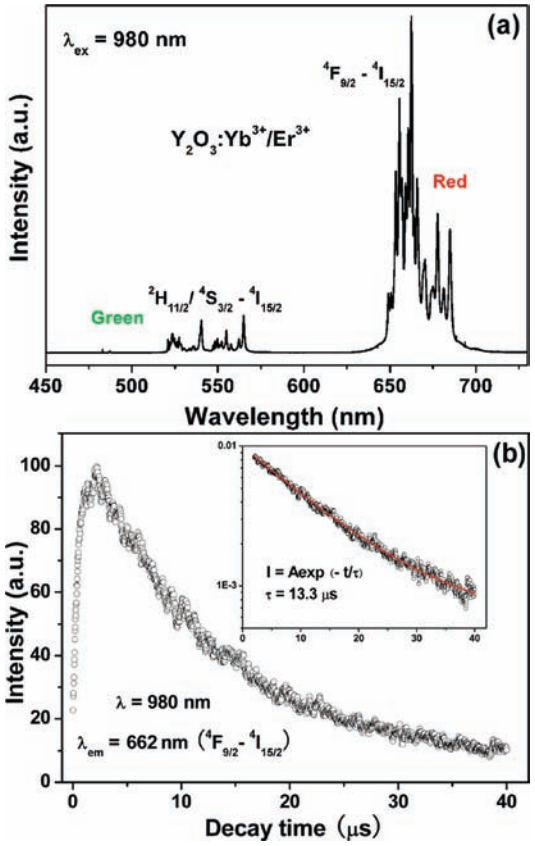

Figure 6. (a) UC luminescence spectra of Y_2O_3:10%Yb^{3+},1%Er^{3+} hollow spheres under 980 nm light excitation and (b) the temporal behavior of Er^{3+} in Y_2O_3:10%Yb^{3+},1%Er^{3+} sample. Inset is the luminescence decay curve of Er^{3+} (662 nm, $^4F_{9/2}-^4I_{15/2}$).

and some weak lines in the longer wavelength region, which are due to the charge-transfer band (CTB) between the O^{2-} and Eu^{3+} ions and the f-f transition of the Eu^{3+} ions, respectively. Upon excitation into the CTB of the Eu^{3+} ions at 248 nm, the emission spectrum exhibits six groups of emission lines, which are ascribed to the $^5D_1-^7F_1$ and $^5D_0-^7F_J$ (J = 0, 1, 2, 3, 4) transitions of the Eu^{3+} ions, respectively. The emission spectrum is dominated by the red $^5D_0-^7F_2$ (610 nm) transition of the Eu^{3+} ions which is an electric-dipole allowed transition and hypersensitive to the environment. Figure 5b shows the decay curve for the luminescence of the $^5D_0-^7F_2$ transition of the Eu^{3+} ions in Y_2O_3 host lattice. The luminescence decay curve of Y_2O_3:Eu^{3+} sample can be well fitted into a single-exponential function, and the lifetime of the Eu^{3+} ions is determined to be 1.47 ms. The result is basically in agreement with other Y_2O_3:Eu^{3+} phosphors in previous reports.[8,20]

The UC luminescence spectrum of Y_2O_3:1%Er^{3+} sample consists of two intense bands in the green emission region and a band in the red emission region (Figure S3 in the Supporting Information). The series of emission lines between 515 and 565 nm can be assigned to the $^2H_{11/2}-^4I_{15/2}$ and $^4S_{3/2}-^4I_{15/2}$ transitions of the Er^{3+} ions, and the band at 662 nm in the red emission region is assigned to the $^4F_{9/2}-^4I_{15/2}$ transition of Er^{3+} ions. Figure 6a shows the UC emission spectrum of Y_2O_3:10%Yb^{3+},1%Er^{3+} sample. The UC luminescence spectrum of Y_2O_3:10%Yb^{3+},Er^{3+} hollow microspheres mainly includes strong red emission corresponding to the $^4F_{9/2}-^4I_{15/2}$ transition of the Er^{3+} ions, together with the weak emissions assigned to the $^2H_{11/2}-^4I_{15/2}$ and $^4S_{3/2}-^4I_{15/2}$ transitions of the Er^{3+} ions, respectively. One can see clearly from the UC emission spectra that the emission color changed greatly when Yb^{3+} ions were codoped with Er^{3+} into Y_2O_3 host lattice. This result (the green emission decreases, and the red emission increases) agrees well with the previous literature.[37−40] The temporal behavior for UC luminescence of Er^{3+} (662 nm, $^4F_{9/2}-^4I_{15/2}$) in the Y_2O_3:10%Yb^{3+},1%Er^{3+} sample was also investigated (Figure 6b). The time evolution process consists of an initial rise starting at zero intensity followed by a decay, which is the feature of an energy-transfer upconversion process.[41] The luminescence decay curve of Er^{3+} (662 nm, $^4F_{9/2}-^4I_{15/2}$) in Y_2O_3:10%Yb^{3+},1%Er^{3+} sample can be well fitted into a single-exponential function, and the lifetime of the Er^{3+} ions is determined to be 13.3 μs (inset in Figure 6b). The result agrees well with other Er^{3+}-doped UC phosphors in the previous literatures.[42]

4. Conclusions

In summary, we have successfully prepared the uniform and well-dispersed Y_2O_3 hollow spheres by a template-directed method with MF microspheres as templates. The as-obtained Y_2O_3:Ln^{3+} (Ln = Eu, Yb, and Er) hollow spheres show strong down- and upconversion luminescence under UV excitation or 980 nm light excitation, which may find potential applications in the fields of lighting, displays, or biomedicine. Furthermore, the main process of this method was carried out in aqueous condition without any organic solvents, surfactant, catalyst, or etching agents. This facile, green, and low-cost method may be of great significance in the synthesis of other hollow spherical or core−shell structured inorganic functional materials.

Acknowledgment. This work is financially supported by the National Natural Science Foundation of China (Grant No. 20771098) and the Fund for Creative Research Groups (Grant No. 20921002), and the National Basic Research Program of China (973 Program, Grant Nos. 2007CB935502 and 2006CB601103).

Supporting Information Available: EDX spectra of precursor and Y_2O_3 hollow microspheres (Figure S1); FT-IR spectra of MF microspheres, precursor, and Y_2O_3 hollow microspheres (Figure S2); UC luminescence spectra of Y_2O_3:1%Er^{3+} hollow spheres under 980 nm light excitation (Figure S3). This material is available free of charge via the Internet at http://pubs.acs.org.

(37) Wang, F.; Liu, X. G. *J. Am. Chem. Soc.* **2008**, *130*, 5642.
(38) Li, Y. P.; Zhang, J. H.; Zhang, X.; Luo, Y. S.; Ren, X. G.; Zhao, H. F.; Wang, X. J.; Sun, L. D.; Yan, C. H. *J. Phys. Chem. C* **2009**, *113*, 4413.
(39) Matsuura, D. *Appl. Phys. Lett.* **2002**, *81*, 4526.
(40) Bai, X.; Song, H. W.; Pan, G. H.; Lei, Y. Q.; Wang, T.; Ren, X. G.; Lu, S. Z.; Dong, B.; Dai, Q. L.; Fan, L. B. *J. Phys. Chem. C* **2007**, *111*, 13611.
(41) (a) Balda, R.; Fernández, J.; Mendioroz, A.; Voda, M.; Al-Saleh, M. *Phys. Rev. B* **2003**, *68*, 165101. (b) Heer, S.; Wermuth, M.; Krämer, K.; Ehrentraut, D.; Güdel, H. U. *J. Lumin.* **2001**, *94−95*, 337. (c) Li, D.; Dong, B.; Bai, X.; Wang, Y.; Song, H. W. *J. Phys. Chem. C* **2010**, *114*, 8219.
(42) (a) Fan, X. P.; Wang, J.; Qiao, X. S.; Wang, M. Q.; Adam, J.; Zhang, X. H. *J. Phys. Chem. B* **2006**, *110*, 5950. (b) Venkatramua, V.; Falcomera, D.; Speghinia, A.; Bettinellia, M.; Jayasankarb, C. K. *J. Lumin.* **2008**, *128*, 811.